IEEE Access
Multidisciplinary | Rapid Review | Open Access Journal

Received December 7, 2018, accepted December 28, 2018, date of publication January 14, 2019, date of current version February 6, 2019.

Digital Object Identifier 10.1109/ACCESS.2019.2892654

Novel Multi-Material 3-Dimensional Low-Temperature Co-Fired Ceramic Base

TAKAHIRO HIRAO[1] AND SHU HAMADA[2]

[1]Components Business Unit, Murata Manufacturing Co., Ltd., Nagaokakyo 617-8555, Japan
[2]Corporate Technology and Business Development Unit, Murata Manufacturing Co., Ltd., Nagaokakyo 617-8555, Japan

Corresponding author: Takahiro Hirao (hirao@murata.com)

ABSTRACT This paper proposes a novel multi-material 3D low-temperature co-fired ceramic base called NeuroStone. It employs 3D inkjet printing with ceramic and copper particle suspension, followed by co-firing. This technology provides both free-form and non-planar electrodes not only on the surface but also inside the device. NeuroStone makes it possible to enhance the directional freedom and electrode packing density in the field of miniature interconnection devices. This report demonstrates that the proposed technology can realize sophisticated shapes of interconnection devices fabricated by additive manufacturing, which can significantly enhance the scope of electronics.

INDEX TERMS Additive manufacturing, ceramic device, direct print, printed electronics, three-dimensional electronics, three-dimensional printing.

A. INTRODUCTION

High electrode packing density and high directional freedom are important in electronic devices like Printed Circuit Board (PCB). Electrode packing density indicates the number of electrodes that can be accommodated on the base, and directional freedom indicates that the electrode has no directional limitation in the device.

Multilayer devices [1] and Molded Interconnect Devices (MIDs) have been developed earlier [2]–[4]. Multilayer devices require a via to electrically connect each layer. The direction of connection using the via is limited only to the vertical direction. On the other hand, an MID cannot have electrodes inside the device. The electrode can be located only on the surface. Despite certain improvements, both technologies eventually have strict limitations on electrode packing density enhancement and directional freedom.

We focused on inkjet and 3D printing technologies to address these limitations [5]–[7] because these technologies have been in existence for several decades and many devices have been developed based on them [8]–[10]. We have studied the possibility of using 3D printing technology in developing a new 3-dimensional low-temperature co-fired ceramic (LTCC) electronic base called NeuroStone^{TM}. NeuroStone^{TM} can facilitate the fabrication of LTCC devices with high electrode packing density and directional freedom (Fig. 1).

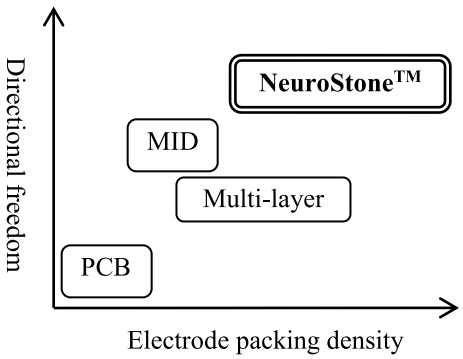

FIGURE 1. Electrode packing density and directional freedom of NeuroStone^{TM} in comparison with other device types.

I. EXPERIMENTAL

A. CAD/CAM PROCESS

NeuroStone^{TM} was designed with commercially available 3D-CAD. The 3D-CAD data corresponded to multiple materials separated by material type, e.g., copper, ceramic, and supporting materials. The 3D-CAD data of each material were exported to the standard triangulated language (STL) format individually; then, the STL data were sliced to a 2D vector format, namely, the multilayer scalable vector graphics (SVG) format. The SVG of each material was converted to the quantized raster images of each layer.

B. INK MATERIAL

We developed inkjet inks for LTCC (BaO-Al_2O_3-SiO_2-MnO-TiO_2), copper, and the supporting material. The inks contained a functional particle having a BET-equivalent particle diameter of 100 nm or more, a dispersing agent, and an organic solvent. The viscosity of the ink was 10–25 mPa·s at the shear rate of 1000 s^{-1}.

C. EXPERIMENTAL SETUP

A schematic diagram of the experimental setup developed by us is shown in Fig. 2. This setup comprises an inkjet unit, a pair of stages, and a pair of drying units. A sample was printed on a stage by the inkjet unit. While a layer of the sample on the stage was in the process of being printed by the inkjet unit, the other sample was dried on another stage by the drying unit. This process was efficient, as it allowed only a short resting time of the inkjet heads. The printing and drying steps were continued until the last layer was printed and dried.

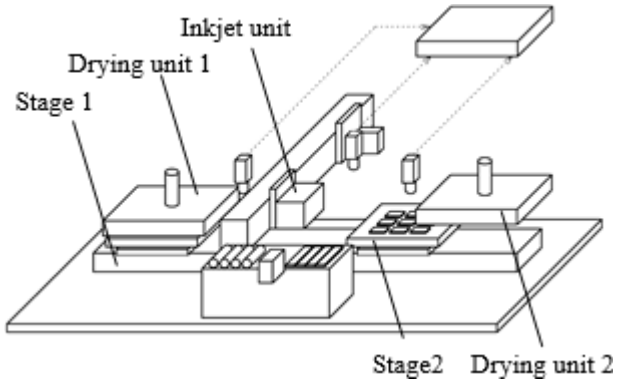

FIGURE 2. Experimental setup.

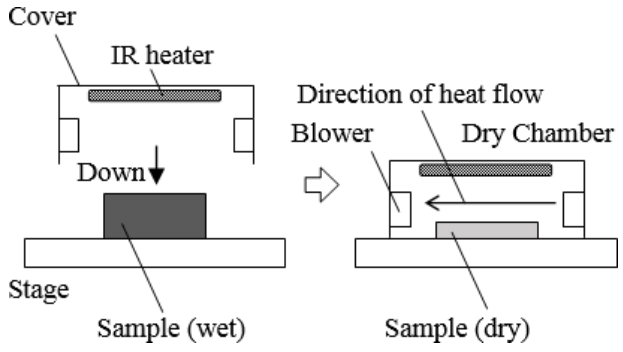

FIGURE 3. Schematic of the drying unit.

In the present work, we used LTCC ink, copper ink, and support material ink. The inkjet heads employed were Xaar1002 (Xaar) and KM1024SHB (Konica Minolta). The inkjet heads were controlled by a GIS controller (Global Inkjet Systems). The printing scheme was as follows: a single layer was printed by the inkjet unit on the stage after heating to 60 °C; the stage was then moved to a position under the drying unit, where the solvent in the ink was evaporated, and finally a thin printed layer was formed. Fig. 3 shows the method adopted for drying. The drying unit comprising an IR heater and a blower descends on the stage. The chamber structure is intended to prevent contamination of the sample.

TABLE 1. Specifications.

X-resolution	1440 dpi
Y-resolution	1440 dpi
Stage size	240 mm × 240 mm
Stage speed	50–100 mm/s
Print dot size	ϕ 30 μm
Layer thickness	2-3 μm

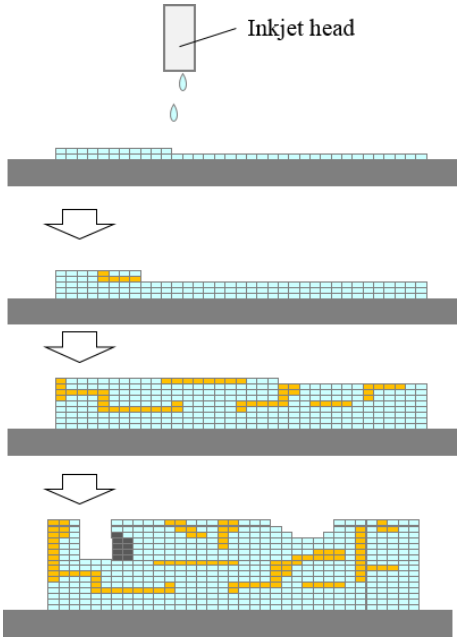

FIGURE 4. Schematic of the 3D printing process.

D. MANUFACTURING PROCESS

The 3D inkjet printing process is shown in Fig. 4. The inkjet print heads concurrently fire droplets of each type of ink from the nozzles toward the stage. Here, light blue color represents the ceramic ink droplet and yellow represents the copper ink droplet. Each ink droplet is deposited on the surface and a thin printed layer is formed after the solvent dries. The stacked multiple layers gradually form a 3-dimensional shape. An undercut shape was previously printed using the support material ink shown in black. The printed raw device was co-fired at 800–1000 °C in N_2/H_2 atmosphere. The support material was dissipated during the co-firing process. In this study, we manufactured various devices of size up to 5 mm × 5 mm with 0.5 mm thickness.

II. RESULTS AND DISCUSSION

A. COMPLEX STRUCTURE AND ELECTRODE ON SURFACE

For demonstration purpose, we fabricated a sample in the shape of a honeycomb. Fig. 5 shows its 3D CAD image and Fig. 6 shows the microscope image. The sample size was 5 mm × 5 mm × 0.5 mm after co-firing. The images show that

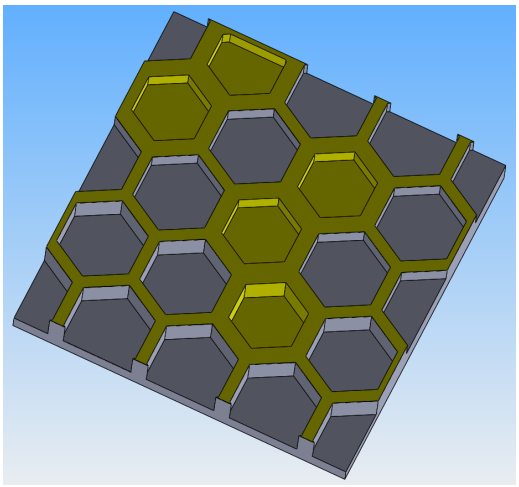

FIGURE 5. 3D image of electrode on LTCC surface.

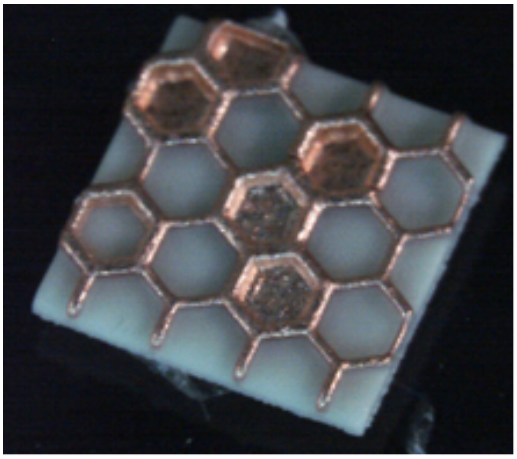

FIGURE 6. Electrodes on LTCC surface (after co-firing).

complex structures such as copper electrodes can be created on the surface of LTCC with this method.

Neither gaps nor cracks were found in this sample, even at the joints between LTCC and copper. We believe there are two reasons for the sample being defect-free. One was the optimum ratio between the quantities of the LTCC material and copper ink to eliminate significant differences between the shrinkage rates of LTCC and copper. The other was the consideration of the shrinkage ratio in the design.

Fig. 7 shows the shrinkage amounts of raw and co-fired samples. The shrinkage ratio was 85 % in terms of the dimensions.

The 3D CAD image (Fig. 8) and co-fired sample (Fig. 9) show that it is possible to create a sloping shape of the ceramics and place the electrode on the sloping surface of the structure. The sample was very accurately produced when compared with the CAD designed shape.

B. UNIQUELY SHAPED ELECTRODE AND EMBEDDED ELECTRODE

We fabricated a uniquely shaped electrode for demonstration purpose. Electrodes in the shape of a copper pipe were

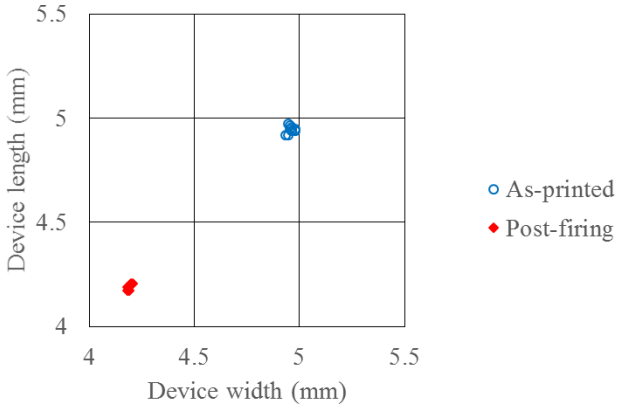

FIGURE 7. Shrinkage of the as-printed and post-firing samples.

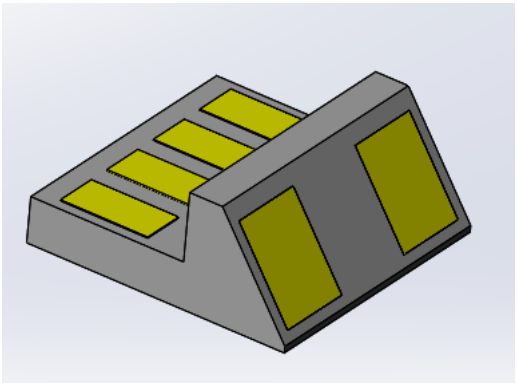

FIGURE 8. CAD design of electrodes on the sloping surface.

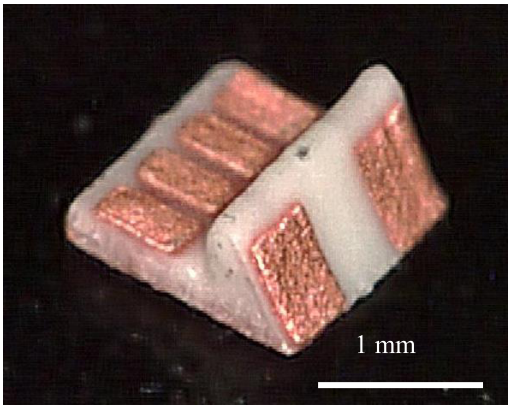

FIGURE 9. Electrodes on the sloping surface (after co-firing).

fabricated inside the LTCC (Fig. 10). The diameter of this tablet-like sample was 4.1 mm.

Fig. 11 shows the transparent X-ray image of the top view of the sample. It is confirmed that the copper pipe electrodes were present inside the LTCC. The black area is the copper pipe electrode. The dark gray area is the LTCC. The light gray area is the cavity. Copper pipe electrodes meet at the center of the sample.

Fig. 12 shows the side view of the X-ray image. The pipe electrode penetrates through the sample. The support material was filled in during printing, and then it was burned off during the co-firing process. This formed the vacancy in the sample.

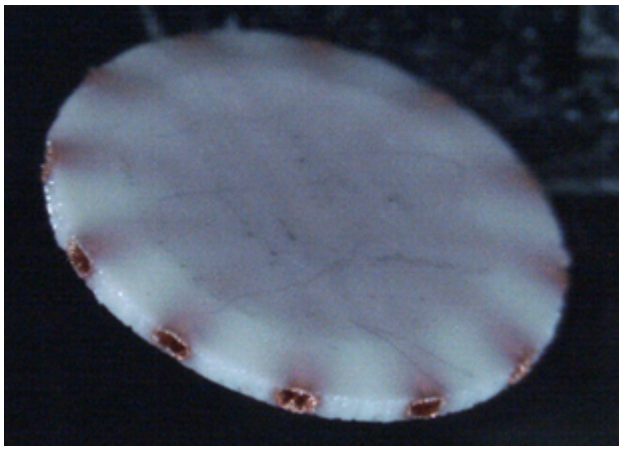

FIGURE 10. Pipe-shaped electrode (after co-firing).

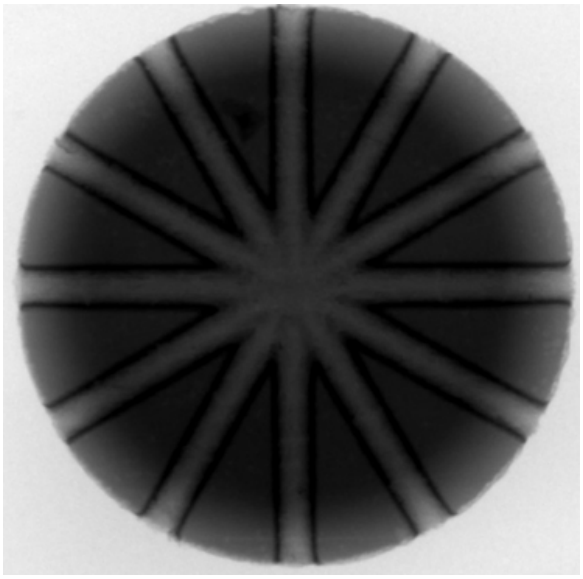

FIGURE 11. X-ray image of pipe-shaped electrode sample.

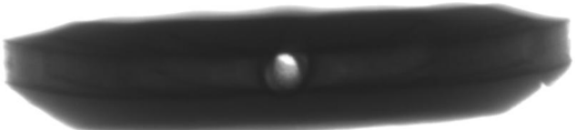

FIGURE 12. Through-hole inside the sample.

These results indicate that this technology can be used to fabricate various unique electrode shapes inside the LTCC.

C. CHARACTERISTICS

1) LINE WIDTH

The electrode width was measured for demonstration purpose. Fig. 13 shows the microscope image of the electrodes. Fig. 14 shows the designed and printed line widths. The data indicate that the printed line widths have linearity with the designed line widths.

2) ELECTRONIC RESISTIVITY

Fig. 15 shows the electronic resistivity using 4-terminal sensing. Nine samples were fabricated to measure the

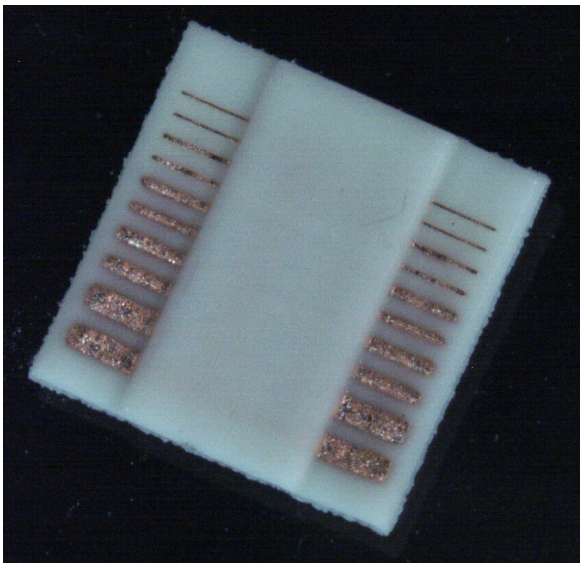

FIGURE 13. Copper electrodes (after firing).

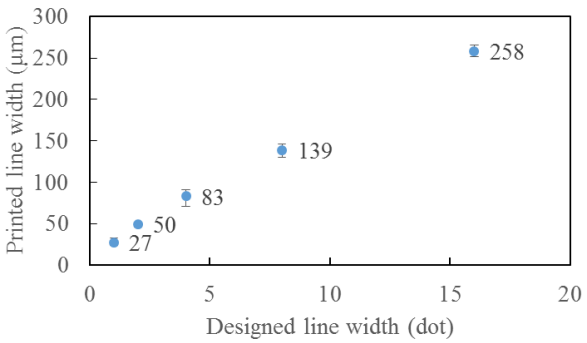

FIGURE 14. Line widths of the electrode.

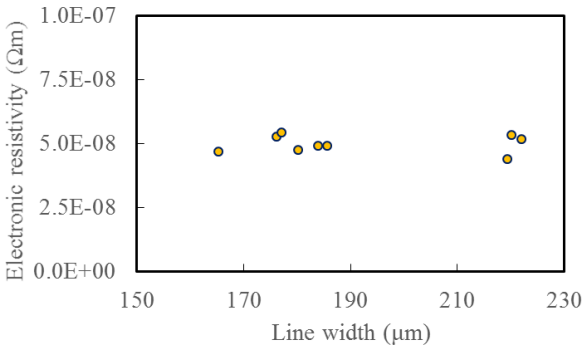

FIGURE 15. Electronic resistivity.

electronic resistivity. These samples had line widths of 165-222 μm, line length of 5 mm, and line thickness of 9 μm. It can be seen from Fig. 15 that NeuroStone^{TM} has sufficiently low electronic resistivity.

III. CONCLUSION

The present work was intended to show the applicability of 3D printing technology to electronic device manufacturing. The results showed that it is possible to achieve high electrode packing density and directional freedom in the

manufacturing process. NeuroStone^{TM} facilitates the direct connection of electrodes without via as opposed to multilayer devices. NeuroStone^{TM} electrodes can be placed not only on the surface but also inside the device, which is not common in MID technology. Additionally, NeuroStone^{TM} allows free-form structure of the co-fired LTCC and copper.

In our future study, we plan to further expand the field of multi-material 3D printing technology of ceramic and metal. For example, we will design new devices with heat and mechanical stress resistance. Furthermore, we plan to accomplish mass manufacturing of the devices. It is necessary to improve the printer and ink to achieve this. In addition, the printing capability should be enhanced and the manufacturability of ink should be scaled up.

REFERENCES

[1] T. He, W. Li, W. Ren, and Z. Xue, "Multi-layer stacked 3D UHF-band miniaturized frequency selective structure," in *Proc. 6th Asia–Pacific Conf. Antennas Propag. (APCAP)*, Xi'an, China, 2017, pp. 1–3, doi: 10.1109/APCAP.2017.8420389.

[2] H. Yun, H. Kim, and I. Lee, "Research of circuit manufacturing for new MID technology development," *J. Mech. Sci. Technol.*, vol. 31, no. 12, p. 5737, Dec. 2017, doi: 10.1007/s12206-017-1115-z.

[3] B. Bachy *et al.*, "Novel ceramic-based material for the applications of molded interconnect devices (3D-MID) based on laser direct structuring," *Adv. Eng. Mater.*, vol. 20, no. 7, p. 1700824, Mar. 2018, doi: 10.1002/adem.201700824.

[4] R. H. Liu, W.-B. Young, and H. P. Ming, "Design of the printing pattern on film for three-dimensional molded interconnect devices," *Adv. Polym. Technol.*, vol. 37, no. 6, pp. 1722–1731, Oct. 2018, doi: 10.1002/adv.21830.

[5] E. MacDonald *et al.*, "3D printing for the rapid prototyping of structural electronics," *IEEE Access*, vol. 2, pp. 234–242, Dec. 2014, doi: 10.1109/ACCESS.2014.2311810.

[6] A. M. Wätjen, P. Gingter, M. Kramer, and R. Telle, "Novel prospects and possibilities in additive manufacturing of ceramics by means of direct inkjet printing," *Adv. Mech. Eng.*, vol. 6, p. 141346, May 2015, doi: 10.1155/2014/141346.

[7] P. J. Brown, M. Ediger, T. Downing, J. Wang, and R. Day, "Where next for industrial digital printing?" in *Proc. NIP, Digit. Fabr. Conf.*, Nov. 2017, no. 1, pp. 206–209.

[8] C. Sternkiker, E. Sowade, K. Y. Mitra, R. Zichner, and R. R. Baumann, "Upscaling of the inkjet printing process for the manufacturing of passive electronic devices," *IEEE Trans. Electron Devices*, vol. 63, no. 1, pp. 426–431, Jan. 2016, doi: 10.1109/TED.2015.2498311.

[9] R. Rammal *et al.*, "Multimaterial inkjet technology for the fabrication of microwave components," in *Proc. Eur. Microw. Conf.*, Nuremberg, Germany, Oct. 2013, pp. 790–793. [Online]. Available: https://ieeexplore.ieee.org/document/6686775

[10] F. Simon, "3D printing technologies for electronics," *J. Imag. Soc. Jpn.*, vol. 56, no. 6, pp. 617–620, 2017.

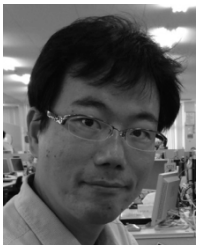

TAKAHIRO HIRAO received the B.S. degree in electronic engineering and the M.S. degree in electronic engineering and computer science from the Shibaura Institute of Technology, in 2000 and 2002, respectively. In 2002, he joined Murata Manufacturing Co., Ltd. His research interest includes electronic components fabricated by additive manufacturing.

SHU HAMADA received the B.S. and M.S. degrees in mechanical engineering from Tohoku University, in 1999 and 2001, respectively.

In 2013, he joined Murata Manufacturing Co., Ltd. His current research interest includes application of additive manufacturing to electronics.